NPS-MAE-23-011

NAVAL POSTGRADUATE SCHOOL

MONTEREY, CALIFORNIA

TRANSFORMATIONAL UUV A.I.
(A SIXTY-DAY STUDY)

by

Timothy Sands

June 2023

Approved for public release. Distribution is unlimited.

Prepared for: OPNAV N2/N6 - Information Warfare.
This research is supported by funding from the Naval Postgraduate School, Naval Research Program (PE 0605853N/2098).
NRP Project ID: NPS-23-N180-A

THIS PAGE INTENTIONALLY LEFT BLANK

REPORT DOCUMENTATION PAGE

PLEASE DO NOT RETURN YOUR FORM TO THE ABOVE ORGANIZATION.

1. REPORT DATE	**2. REPORT TYPE**	**3. DATES COVERED** START DATE	END DATE
June 8, 2023	Technical Report	October 20, 2022	June 8, 2023

4. TITLE AND SUBTITLE

Transformational UUV A.I. (A Sixty-Day Study)

5a. CONTRACT NUMBER	**5b. GRANT NUMBER**	**5c. PROGRAM ELEMENT NUMBER**
		0605853N/2098
5d. PROJECT NUMBER	**5e. TASK NUMBER**	**5f. WORK UNIT NUMBER**
NPS-23-N180-A		

6. AUTHOR(S)

Timothy Sands

7. PERFORMING ORGANIZATION NAME(S) AND ADDRESS(ES)	**8. PERFORMING ORGANIZATION REPORT NUMBER**
Naval Postgraduate School 1 University Circle Monterey, CA, 93943-5000	NPS-MAE-23-011

9. SPONSORING/MONITORING AGENCY NAME(S) AND ADDRESS(ES)	**10. SPONSOR/MONITOR'S ACRONYM(S)**	**11. SPONSOR/MONITOR'S REPORT NUMBER(S)**
Naval Postgraduate School, Naval Research Program; OPNAV N2/N6 - Information Warfare	NRP; N2/N6	NPS-23-N180-A

12. DISTRIBUTION/AVAILABILITY STATEMENT

Approved for public release. Distribution is unlimited.

13. SUPPLEMENTARY NOTES

14. ABSTRACT

Unmanned vehicles necessitate extreme autonomy by the nature of being unmanned. Onboard systems must sense, decide, and act with minimal or no human interaction. This manuscript elaborates the brief, sixty-day study of recent autonomy developments for unmanned underwater vehicles beginning with a rigorous review of very recent literature and culminating with initial efforts to create computer simulations in MATLAB®/SIMULINK® of the recent seminal publication of deterministic artificial intelligence. The methods were developed for highly nonlinear circuits and later extended to spacecraft guidance and control before recently being developed for unmanned underwater vehicles. Mathematical expressions of the governing physics are used to formulate self-awareness statements, where optimal learning is used to discern unknown or unknowable properties. Critical analysis and selection of discretization and differential equation solvers is offered using numerical precision as the key figure of merit for selection. Machine precision of the utilized software version was achieved in validating simulations, where the simulation illustrated autonomous navigation without any kind of controller tuning. Recommendations are offered for future studies utilizing the developed simulation environment.

15. SUBJECT TERMS

Multi-spectral remote sensing; active and passive microwave remote sensing; spaceborne platforms; remote sensing applications; meteorology; bio–radar; C–band; on-orbit satellite storage; signal processing

16. SECURITY CLASSIFICATION OF: a. REPORT	b. ABSTRACT	C. THIS PAGE	**17. LIMITATION OF ABSTRACT**	**18. NUMBER OF PAGES**
U	U	U	UU	43

19a. NAME OF RESPONSIBLE PERSON	**19b. PHONE NUMBER** *(Include area code)*
Timothy Sands	831-656-3201

STANDARD FORM 298 (REV. 5/2020)
Prescribed by ANSI Std. Z39.18

THIS PAGE INTENTIONALLY LEFT BLANK

NAVAL POSTGRADUATE SCHOOL
Monterey, California 93943-5000

Ann E. Rondeau
President

Scott Gartner
Provost

The report entitled "Transformational UUV A.I (A Sixty-Day Study)" was prepared for OPNAV N2/N6 - Information Warfare and funded by Naval Postgraduate School, Naval Research Program (PE 0605853N/2098).

Further distribution of all or part of this report is authorized.

This report was prepared by:

SANDS.TIMOTHY.ANDREW.1056639299
Digitally signed by SANDS.TIMOTHY.ANDREW.1056639299
Date: 2023.11.23 09:29:28 -05'00'

Timothy Sands
Professor of the Practice

Reviewed by:

BINGHAM.BRIAN.STEVEN.1504993910
Digitally signed by BINGHAM.BRIAN.STEVEN.1504993910
Date: 2023.11.27 10:34:24 -08'00'

Brian Bingham, Chairman
Department of Mechanical and Aerospace Engineering

Released by:

SMITH.KEVIN.B.1230026366
Digitally signed by SMITH.KEVIN.B.1230026366
Date: 2023.12.06 15:39:46 -08'00'

Kevin B. Smith
Vice Provost for Research

THIS PAGE INTENTIONALLY LEFT BLANK

ABSTRACT

Unmanned vehicles necessitate extreme autonomy by the nature of being unmanned. Onboard systems must sense, decide, and act with minimal or no human interaction. This manuscript elaborates the brief, sixty-day study of recent autonomy developments for unmanned underwater vehicles beginning with a rigorous review of very recent literature and culminating with initial efforts to create computer simulations in MATLAB®/SIMULINK® of the recent seminal publication of deterministic artificial intelligence. The methods were developed for highly nonlinear circuits and later extended to spacecraft guidance and control before recently being developed for unmanned underwater vehicles. Mathematical expressions of the governing physics are used to formulate self-awareness statements, where optimal learning is used to discern unknown or unknowable properties. Critical analysis and selection of discretization and differential equation solvers is offered using numerical precision as the key figure of merit for selection. Machine precision of the utilized software version was achieved in validating simulations, where the simulation illustrated autonomous navigation without any kind of manual controller tuning.

THIS PAGE INTENTIONALLY LEFT BLANK

TABLE OF CONTENTS

I. INTRODUCTION 1

A. LITERATURE REVIEW 1

1. Review of the current state of research field 2

a. Operational developments 2

***b. Cooperation*..... 3**

***c. Design*..... 4**

***d. Localization and positioning*..... 5**

2. Reinforcement learning 8

***a. Swarms*..... 9**

***b. Heterogeneous formations*..... 9**

3. Deterministic artificial intelligence 10

II. MATERIALS AND METHODS 12

1. Governing physics differential equations 12

2. Deterministic artificial intelligence self-awareness statements 15

3. Deterministic artificial intelligence optimal learning 16

4. Discretization and numerical precision 17

III. RESULTS 18

A. DISCUSSION 20

1. Recommended future research 20

2. Patents 21

APPENDIX A 23

LIST OF REFERENCES 25

INITIAL DISTRIBUTION LIST 29

THIS PAGE INTENTIONALLY LEFT BLANK

LIST OF FIGURES

Figure 1. Unmanned underwater vehicle employment. 1
Figure 2. Unmanned underwater vehicle employment benchmarks. 2
Figure 3. Preliminary results using deterministic artificial intelligence with learning 11
Figure 4. MATLAB®/SIMULINK® simulation topology. 12
Figure 5. Comparison of numeric precision 18
Figure 6. Validating maneuvering simulation 19
Figure 7. Euler’s moment equation subsystem in Figure 4. 23
Figure 8. Newton’s translation equation subsystem in Figure 4. 23
Figure 9. Rotational kinematics subsystem in Figure 4. 23
Figure 10. Attitude controller subsystem (self–awareness statements) in Figure 4. 23
Figure 11. Attitude controller subsystem (optimal learning) in Figure 4. 24

THIS PAGE INTENTIONALLY LEFT BLANK

LIST OF TABLES

Table 1. Table of proximal variable and acronym definitions. 13
Table 2. Table of proximal variable and acronym definitions. 14
Table 3. Table of proximal variable and acronym definitions. 15
Table 4. Table of proximal variable and acronym definitions. 15
Table 5. Table of proximal variable and acronym definitions. 16
Table 6. Ordinary differential equation stiffness 17
Table 7. Numerical precision for different solver schemes using MATLAB® R2022B 18

THIS PAGE INTENTIONALLY LEFT BLANK

I. INTRODUCTION

A. LITERATURE REVIEW

Autonomy advancements are the broad context of the study described in this manuscript. Such advancements are important enablers of operations at sea, such as search and rescue (amongst others), where life-and-death circumstances are possible eventualities (see Figure 1). The purpose of this work is primarily to review the very latest developments in the field to establish the current state of the art (with a specific, slight emphasis on reinforcement learning), but is also to highlight promising methods for future developments.

(**a**)

(**b**)

Figure 1. Unmanned underwater vehicle employment: (a) In the Sea of Japan an MK 18 MOD 2 Kingfish is prepared for deployment during Exercise Noble Vanguard in May 2022 (image credit U.S. Navy, MC2 Pickett, [1]), and (b) Remote demonstration of autonomous operations in Bethesda, Maryland, USA, at the US Naval Surface Warfare Center, Carderock Division [2].

Developments using stochastic artificial intelligence methods [3] are introduced, as well as deterministic artificial intelligence as an emerging, divergent hypothesis. Scientists and engineers outside the field may benefit from a thorough explanation of deterministic artificial intelligence, and the method is therefore elaborated in Section 2, "Materials and Methods." The method is also simulated in Section 3 so that it may be compared to the classical, optimal methods used to produce Figure 2, which depicts autonomous mission execution through minefields.

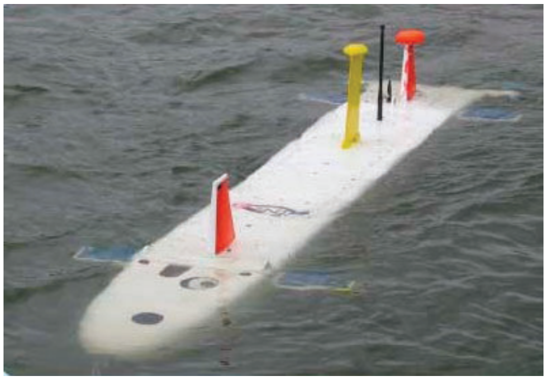

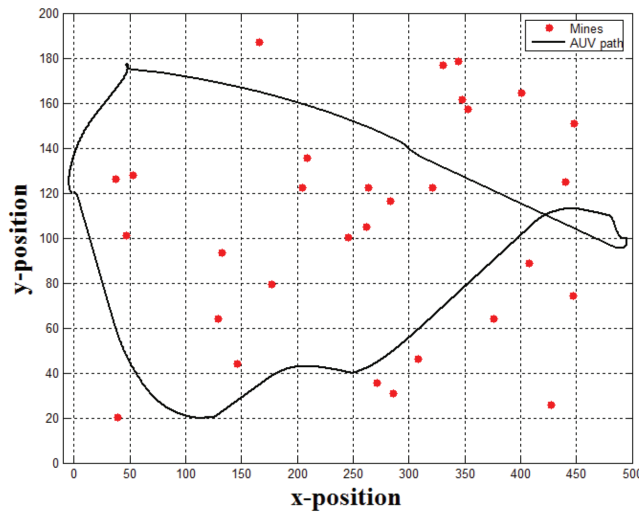

(**a**) (**b**)

Figure 2. Unmanned underwater vehicle employment benchmarks.
(a) Phoenix vehicle from the development of deterministic artificial intelligence in reference. (b) Benchmark task: avoidance of mines while navigating in realistic ocean currents [4].

1. Review of the current state of research field

The review is loosely organized to present operational innovations first, followed by developments key to cooperative interoperability, then design developments, and finally advances in localization and positioning. The review of reinforcement learning is presented, somewhat unusually, as Section 2 to serve readers who scan the manuscript with a primary interest in reinforcement learning developments.

a. Operational developments

Unmanned underwater vehicles share maritime information and data comprising domain awareness [4]–[5]. Yang [6] analyzed signal properties of communications channels under various random conditions, including surface waves in shallow waters, and hypothesized reasons for loss of coherence in phase and amplitude variations and individual path's temporal coherence. According to Sinisterra, information sharing facilitates utilization of unmanned underwater vehicles as mother ships for unmanned aerial vehicles executing surveillance and sensing missions [7]. Allard et al. [8] elaborated on two vehicles collaboratively employing systems for imaging based on bistatic lasers autonomously to image ocean bottoms, a process enhanced by a novel "M-hull" design for unmanned surface vehicles. As an alternative to laser systems, acoustic channels can be used; Cen et al. [9] identified that the key dynamics of such channels are driven by coding rate, modulation method, and transmission power, allowing adaptive prediction of the states of channels for double-scale adaptive signal transmission. Collaborative navigation while minimizing collisions necessitates short-range transmission through the sea, and Savkin et al. illustrated a law utilizing sliding-mode navigation which was validated computationally in [10].

Controlling multilink manipulators attached to unmanned underwater vehicles operating on the dynamic position of objects on the seafloor has recently been proposed by Konoplin et al., using a multi-level system with machine-vision systems to generate point clouds to aid locating and shape-determination [11]. Simulations validated high efficiency sensor information processing. Addressing rapidity and maneuverability challenges encountered during gas and oil pipeline or seabed fiber cable repair, in 2022, Liu et al. [12] used numerical models to investigate vehicle hydrodynamic performance focusing on the propeller interaction with the hull; one finding was strong coupling where performance tended towards stability.

b. Cooperation

Cooperation between unmanned surface vehicles and unmanned underwater vehicles can be facilitated by acoustic communications. Since unmanned surface vehicles have a relatively wider range, they are more efficient at tracking unmanned surface vehicles compared to vice versa. Kang et al. [13] proposed an algorithm usable by unmanned surface vehicles for tracking unmanned underwater vehicles, consisting of an extended Kalman filter, pattern-based re-searching, and multi-mode guidance. The algorithm proved to be stable and efficient at tackling (in simulated environments) underwater communications environments that are quite complex, where experimental validation was performed in sea trials.

Kotis et al. [14] investigated autonomous swarm formations of unmanned underwater vehicles, paying particular attention to interoperability and cybersecurity as they relate to water variety, velocity, volume, and data transmission veracity with necessarily low bitrates as applied to operations for search-and-rescue. Yan et al. [15] proposed approaches for swarm formation control, including collision avoidance in disturbance environments (e.g., currents and waves). One approach proposed included using a disturbance observer based on a sliding mode for identification of dynamic disturbances. Another option was inclusion of an artificial potential function in the collision avoidance control law, the stability of which was illustrated by boundedness of errors in accordance with Lyapunov theorem where Barbalat's lemma is used to illustrate convergence.

Yun et al. proposed having the unmanned underwater vehicle be towed by an unmanned surface vehicle, where wired communications can provide higher speed communications and stable power supply [16]. Seeking to address weak signals, amongst other complications, Wang et al. proposed a gated recurrent unit network with a cubature Kalman filter [17]. The proposed network is trained using the filter gain, prediction error, and filter innovation, where learning is used to predict the current target state, and tracking prediction is converted to a problem of time-series prediction for target motion uncertainty resolution. Stability and accuracy improvements were validated in simulation experiments. A high-gain observer was proposed by Yan et al. for adaptive formation control, including collision avoidance, using radial basis functions to estimate unknown disturbances; stability was evaluated using the theorems of Lyapunov [18]. Zhu et al. proposed fractional-order control for transient robustness of depth control, based on the genetic algorithm, fuzzy control, and fractional calculus [19]. Experiments were presented to verify effectiveness and robust steady-state and dynamic performance.

Swarming, multiple, dissimilar vehicles were investigated by Wu et al. who proposed addressing vehicle allocation using a consistency algorithm to develop an extended, dynamic consensus-based bundle algorithm [20]. Multiple tasks were allocated to each unmanned vehicle in a task-matching matrix and cost functions, while reward and marginal utility functions were used to establish vehicle paths and travel times amidst communications constraints. Optimization of vehicle load balances was expressed in discrete time. Simulation experiments were presented merely to validate algorithm speed and efficiency.

c. Design

Several subsystem technologies suggest improvements in power generation, noise reduction, vibration reduction and hydrodynamic efficiency. For example, ocean currents encountered during operations may be used for in situ power generation. Wang et al. introduced a model of coupling between vehicle hulls and a counter-rotating turbine [21].

A sliding-grid method was used to analyze characteristics of surrounding flow and yaw moments during generation of power. Drift angle effects on the counter-rotating turbine were also assessed, where fourteen percent increased longitudinal drag was discerned despite negligible change in the surrounding flow field, while the variation in hydrodynamic coefficients was seven percent. Yaw moments were increased as well. Hull stability in the moored state was not reduced by the counter-rotating turbine, but the turbine performance was impacted greatly at drift angles greater than fifty percent, where thrust and power coefficients were respectively raised by over seventeen percent and over thirty-five percent.

Chen et al. used computational fluid dynamics to study the unsteady flow field and sound field of ducted propellers at four disparate speeds, revealing that inflow condition strongly relates to noise radiated underwater and flow structure of the water [22]. As vehicle speed increased, ducted propeller propulsion efficiency initially rose, then fell. Simulations matched experiments very closely: 0.1% difference in thrust and 0.5% difference in power. The optimal speed happened to also coincide with the minimum hydrodynamic noise, while the importance of turbulent noise increased with navigation speed. Noise and vibration reduction are key to detecting targets underwater with high resolution estimation of direction of arrival, detection distance, and noise rejection. Xu et al. proposed a virtual (large aperture) array comprised of many smaller aperture arrays spread across swarms of unmanned underwater vehicles [23]. Data processing and analysis is complicated by unobserved and corrupted samples, so matrix completion techniques were recommended to recover the corrupted or unobserved data based in the virtual array. The traditional direction of arrival methods seemingly may be employed for bearing estimation using the recovered matrix. Simulations presented in [23] indicate restoration of high resolution and precision. Target recognition, positioning, and navigation may also be facilitated by using low-cost cameras.

d. Localization and positioning

A review of literature on vision-based positioning and navigation was provided in [24] by Qin et al. divided into two categories of state-of-the-art methods: deep-learning based, and geometry-based methods, where the cited reference presented a comparison of the two methods experimentally using a public underwater dataset. *Deep-learning methods* *were seen to produce images five hundred percent faster than geometric-based methods.* Lambertini presented a prototype system named "Blucy" to derive accurate digital replicas of unobserved environments with a goal of creating digital twins for georeferenced underwater surveys [25]. Khawaja et al. provided another, broader survey of unmanned vehicles (both underwater and aerial vehicles) including challenges and threats plus countermeasures against the threats [26]. Amongst the countermeasures was detection, tracking, and classification. Recommended for future development were two additional concepts: employment of unmanned underwater vehicles on the ocean's surface with radio beacons, and establishment of sensor networks with cognitive acoustic and software-defined sonar networks for the detection and tracking of other vehicles.

Small, low-cost side–scan sonar was recommended by Xie et al. for both unmanned underwater and surface vehicles to provide wide coverage and high resolution, particularly when bathymetric data is not available [27]. Data reconstruction using global optimization with a sinusoidal representation network was used in [27] to represent the albedo and beam profile, with modeling of Lambertian scattering used for joint estimation. Using high resolution multi-beam echo sounders yielded bathymetry errors on the order of twenty centimeters aiding unmanned surface or underwater vehicles navigation in shallow water.

Environmental noise susceptibility, low resolution, and slow refresh rate challenge the use of acoustic devices for localization amidst complex terrain, rapid electromagnetic wave attenuation, uncertainties, and disturbances. Furthermore, illumination condition changes, sparse features and phenomena like scattering interfere with visual sensors used for creating depth maps. The combination of an inertial measurement unit with a light detection and ranging camera was proposed by Yang et al. to generate depth maps [28]. The bundle adjustment method was suggested to recalculate the rotation matrix utilizing sensor fusion for prediction of positioning of other vehicles. Reference trajectories in a tank were provided by an ultra-wideband positioning system that proved experimentally to be robust and stable.

Waypoint tracking in strong disturbances can be attempted using machine learning-based control as suggested by Sola et al. [29] who used a soft actor–critic algorithm with deep reinforcement learning that is entropy-regularized. In [29], comparisons were made against a benchmark classical controller comprised of proportional, integral, derivative components. The proposed method proved capable of simultaneously exploring the environment and managing waypoint tracking, where validation was provided using an unmanned underwater vehicle simulator. Software in the loop simulations were also utilized by Zhang et al. to integrate models, motion controllers, sensors, and programming interfaces for task scheduling, swarm formation control, and path planning [30]. Seeking to simultaneously perform well in the cross-domain environments on the surface and sub-surface, Shi et al. designed a vehicle with four hydrofoils capable of silent diving using a vertical propeller and high-speed surface navigation with a water jet propeller with hydrofoils for improved stability and speed [31]. Experiments illustrated fourteen knots surface sailing speed by an unmanned under-water vehicle.

Magnetic sensor accuracy improvements were proposed by Listewnik et al. based on polynomial regression infrastructure modeling in three dimensions [32]. Ultrasonic sensing was proposed to be countered by a novel smart vehicle skin that controls reflected signals [33]. Two–dimensional reflection experiments validated sound absorption up to 28.6 decibels. Acoustic underwater communications between surface and sub-surface vehicles were presented by Kang et al. who proposed augmentation by smoothing of an extended Kalman filter for the surface vehicle's tracking of the sub-surface vehicle [34].

Alrayes et al. recommended enhanced classification and secured communications between surface and subsurface vehicles using artificial intelligence [35]. Facilitating the necessarily large data requirements, Cho et al. [36] passed large amounts of information (camera and sonar data) between two vehicles using an umbilical cord that simultaneously provided electrical power. Validation was offered in [36] using a catamaran–type surface vehicle and torpedo–shaped undersea vehicle utilizing waypoint guidance tracking with sonar and underwater cameras. Raigoza elaborated ubiquitous utility of waypoint guidance for precision-vehicle-trajectory tracking with autonomous collision avoidance [37], while navigation tracking in such algorithms was proven susceptible to computational rate and discretization of actuator controllers.

In [38], Bourgeois et al. describe the efforts of the U.S. Naval Research Laboratory for development in these technologies, particularly applied to teaming of unmanned underwater vehicles [39]. Following the publication of [40], utilizing autonomous unmanned vehicles for under-ship inspection, Eldred et al. [41][42] described a novel spherical vehicle invention: implementation after construction of a novel design called wreck–interior exploration vehicle (WIEVLE) for unique shipwreck interior exploration using open-loop control testing that demonstrated stable four-degree-of-freedom maneuvering capability. Using tethered communications, the vehicle could secure itself to the seabed, release an anchor, and passively loiter at length. Sea trials performed by Eldred et al. validated performance in three types of seabed sediment under varying conditions.

Thus far within this broad review of the literature for unmanned underwater vehicles, developments in operational features, cooperation, design, and localization or positioning have been reviewed and presented where the review emphasized developments in the past 1–2 years.

2. Reinforcement learning

A particular focus on reinforcement learning follows: reinforcement learning is highlighted in this section, while the novel introduction of deterministic artificial intelligence is presented in section 3, followed immediately by validations by simulation in section II., "Methods and Materials." Machine learning paradigms are generally categorized in three manners: supervised learning, unsupervised learning, and reinforcement learning, which often uses recursive instantiations of Bellman's equation to maximize a declared reward function. Utilization of reinforcement learning for underwater mapping was seminally proposed using robot teams in [40]. Although millions of samples are usually required for deep reinforcement learning, the method in [40] was illustrated to be faster than a benchmark lawnmower trajectory method. Asynchronous multithreading proximal policy optimization was proposed by Miller et al. for path planning and trajectory tracking of unmanned underwater vehicles [44]. The methods were applied to different scenarios necessitating offline training to produce autonomous capabilities for planning, tracking, and obstacle avoidance. Reward sparsity was avoided by using a so–called reward-shaping trick, refining the reward at each timestep.

Multi-agent deep reinforcement learning was suggested by Wang et al. for cooperative target capture, using a swarm of unmanned underwater vehicles in dynamic adversarial environments, where polar coordinate control indicators were selected as angular spacing, while the desired capturing radius was subsequently converted to Cartesian coordinates [45]. Dynamics allocation was performed adaptively, and adversarial training was required. Claimed results were mild: the unmanned underwater vehicles were able to form a circular formation near the target without collision. Trajectory tracking was alternatively presented using a line-of-sight algorithm with fixed look-ahead distances. Seeking to overcome limitations of such algorithms, Wang et al. proposed reinforcement learning guidance using an adaptive line-of-sight [46]. Experiments in Tuandao Bay validated path tracking of a Sailfish autonomous underwater vehicle and also validated performance improvements over nominal line-of-sight approaches, where a short-term memory neural network was used to pre-train the reinforcement learning algorithm, and optimization was performed using a deterministic policy gradient.

a. Swarms

Swarms of autonomous vehicles must simultaneously track targets while maintaining swarm formation, and Wang et al. utilized a search method based on deep deterministic policy gradient using both temporal and spatial data with specialized reward function. Success rates were improved twenty percent in simulations. [47] Another optimization alternative is utilization of the Hamilton–Jacobi–Isaac equation as proposed by Duan et al. for tracking control using reinforcement learning, where vehicle dynamics are not known [48]. The simulations presented validated algorithm convergence in about ten seconds. Target localization was proposed by Masmitja et al. using single-beacon range-only methods and improvements were claimed over ultra–short and long–baseline benchmarks using reinforcement learning to find the optimal path that manifest seventeen percent less error than analytically calculated trajectories [49].

b. Heterogeneous formations

Search and tracking can be enhanced by integrating with autonomous aerial vehicles, where maneuvering decisions and perception of situational information remains key. Improvements suggested by Cao et al. incorporated a convolutional neural network (to process high-dimensional situations) and reinforcement learning (for environment interaction training), where game theory's mini-max method was used to solve the Nash equilibrium [50]. Networking vehicles together using wireless technology was studied by Bu et al. who formulated an integer nonlinear problem minimizing consumed energy and age-of-information using a model-free, online, off-policy reinforcement learning method called the deep Q-network algorithm [51]. Numerical simulations were presented in [51], but merely validated convergence, and reduced energy and age of information. Lu et al. proposed vehicle stabilization when seeking to interact with other undersea objects using domain randomization by reinforcement learning with varying payloads and unknown dynamics. This method necessitated fewer samples for training, but errors merely converge to roughly two meters [52].

The literature review thus far is less than impressive regarding the performance of stochastic artificial intelligence applied to autonomous underwater vehicles including reinforcement learning. Accordingly, examination of deterministic artificial intelligence follows and is further elaborated in "Materials and Methods."

3. Deterministic artificial intelligence

Open-loop, feed-forward control is a logical starting point to limit the computational burden of the initially designed control system. Seeking to expand the mission of unmanned vehicles to include object grasping and manipulation, an adaptive or learning paradigm is necessary (augmenting the open-loop, feedforward control), albeit still constrained to slight computational burden. The architectures for robotic learning control are well understood for use in unstructured environments [53], leading to the recent proposal for so-called deterministic artificial intelligence. Five-degree-of-freedom control with optimal learning is a potential next step in the evolution of modern approaches. The approach might have the potential to provide transformational capabilities, but the nascent approach is not yet validated in challenging unknown and/or unstructured environments.

Using system identification, or alternatively the governing physics equations, to substantiate self-awareness statements form the initiation of the recently proposed method called deterministic artificial intelligence [54]. Thus, the first step towards augmenting the current state of the art is to augment the statements of self-awareness to include disturbance environments of forces and torques. Emphasizing feedforward prior to feedback requires prescription of desired trajectory expression, and two prescription methods predominate in the literature: sinusoidal [55] and fuel-minimizing trajectory generation [56]. Since ordinary differential equations have exponential solutions which can be expanded as sums of transcendental sinusoids using Euler's formula, use of such functions is justified as the structural form of commended desired trajectories.

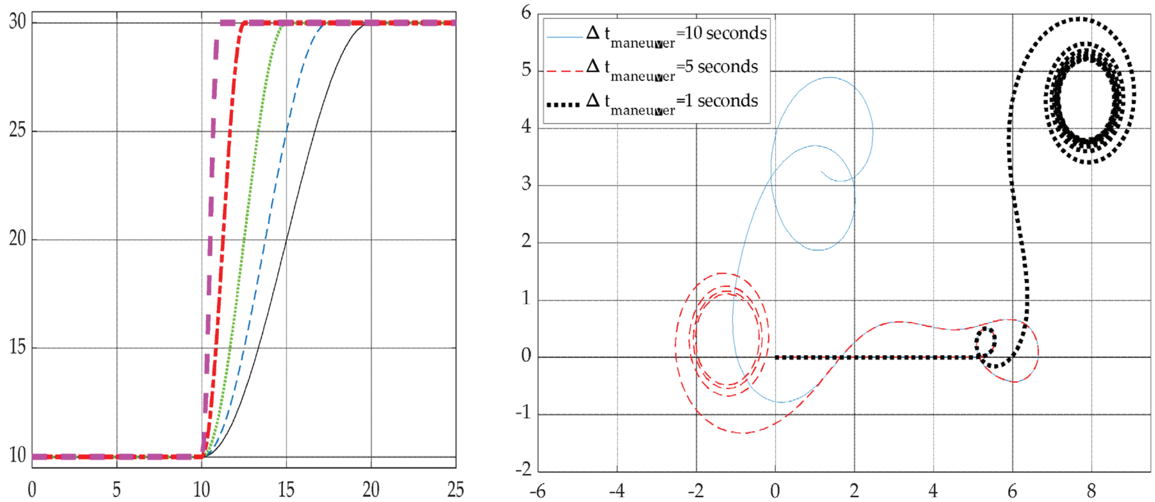

(**a**) (**b**)

Figure 3. Preliminary results using deterministic artificial intelligence with optimal learning [4]: (a) Maneuver angle (degrees) on the ordinant versus time (seconds) for a Phoenix vehicle using development of deterministic artificial intelligence, (b) Validating tight–turn maneuvering while navigating in realistic ocean currents [54].

II. MATERIALS AND METHODS

Carrying forward the notion of deterministic artificial intelligence in the face of unimpressive performances of stochastic methods, subsection II.1. expresses the governing differential equations representing the related laws of physics (e.g., those of Newton, Euler, etc.). These mathematical representations are used to formulate vehicle self–awareness in subsection II.2., while optimal learning of unknown parameters is elaborated in subsection II.3. The complete system topology is displayed in Figure 4; corresponding equations belonging to each subsystem are described in the figure caption. The topology is a screenshot of the SIMULINK® simulation used to produce the results later presented in section III., "Results." While the original development of deterministic artificial intelligence for unmanned underwater vehicles presented in [50] merely elaborated five degrees of mechanical motion (where depth control was merely assumed), the simulation developed in section II and used in section III articulate *for the first time* the seminal six degrees of mechanical motion manifestation.

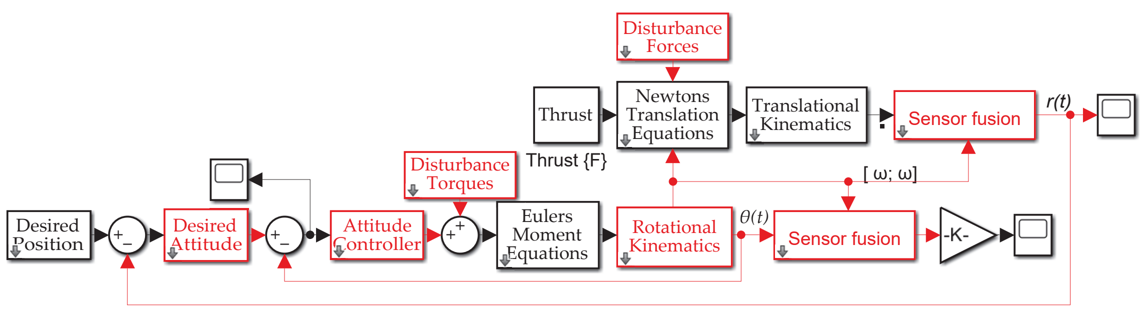

Figure 4. MATLAB®/SIMULINK® simulation topology, where the desired position and attitude are user-provided inputs.
The attitude controller subsystem contains equations (10) and (11), while equation (4) is contained in the Euler's moment equations subsystem, equations (5) – (8) are contained in the rotational kinematics subsystem, equation (3) is contained in subsystem labeled Newton's translational equations. Disturbance forces and torques are simplified as sinusoids. Only the desired attitude is necessary for motion control.

1. Governing physics differential equations

Six-dimensional mechanical motion is manifest as three degrees of rotational motion plus three degrees of translation motion expressed respectively by Euler's moment equations **Error! Reference source not found.** and **Error! Reference source not found.** and Newton's law expressed in equations **Error! Reference source not found.**) and

Error! Reference source not found.). The kinematics relationship in equations (5)–(7) and (8) allow the necessary expressions relative to a non-rotating, non-accelerating reference frame to be transformed into coordinates of rotating reference frames, so that operators have access to motion expressed in terms of their particular preferred reference frame (e.g., body frame, sensor frame, etc.).

$$F|_{inertial} = ma|_{inertial} = m\dot{v}|_{inertial} = m\ddot{x}|_{inertial} \tag{1}$$

$$\tau_{inertial} = J\alpha|_{inertial} = m\dot{\omega}|_{inertial} \tag{2}$$

Variable / acronym	Definition
$F\|_{inertial}$	Vector sum of external forces expressed in non–accelerating, non–rotating coordinates
$a\|_{inertial}$	Acceleration expressed in non–accelerating, non–rotating coordinates
$\dot{v}$	Timed rate of change of velocity expressed in non–accelerating, non–rotating coordinates
$\ddot{x}\|_{inertial}$	Twice differentiated position expressed in non–accelerating, non–rotating coordinates
m	Mass (matrix of nine elements)
$\tau_{inertial}$	Vector sum of external torques expressed in non–accelerating, non–rotating coordinates
J	Mass moments of inertia (matrix of nine elements)
$\alpha\|_{inertial}$	Acceleration expressed in non–accelerating, non–rotating coordinates
$\dot{\omega}\|_{inertial}$	Angular velocity rate of change expressed in non–accelerating, non–rotating coordinates

[1] Such tables are offered throughout the manuscript to aid readability.

Table 1. Table of proximal variable and acronym definitions.

Equations (1) and (2) respectively represent Newton's Law for translation and Euler's moment equations for rotation, where motion is expressed in the coordinates of a non-rotating, non-accelerating reference frame of arbitrary location. Since operators need to express operations in coordinates of a meaningful reference frame often placed for convenience (e.g., a reference frame fixed in the vehicle's body). Expressing motion (both translational and rotational) in coordinates of the preferred frame of reference modifies equations (1) and (2) through the so–called transport theorem (equation (7) in [56] and equation (1) in [58]) leading to equations (3) and (4).

While equations (1)–(4) elaborate the kinetics, the field of dynamics comprises both kinetics and kinematics which provides disparate expressions of the vehicle's attitude. Attitude kinematics are elaborated in equations (5)–(8) including matrices of direction cosines, Euler angles, and quaternions. Direction cosines express the orientation of a vector, while Euler angles imposes a specific paradigm to produce at least three orientation angles permitting expression of three degrees of freedom of rotational motion. Euler angles are ubiquitously preferred by operators familiar with "roll," "pitch," and "yaw" angles to respectively express attitude angles with respect to the vehicle's longitudinal axis, the wings, and the vertical. Since the calculation of these preferred Euler angles contains mathematical singularities, a four-dimensional representation is often used to negate the issue of singularities, and that four-dimensional representation is called the quaternion, and consists of a single real variable and three imaginary variables.

$$F = m\ddot{x} + m\frac{d\omega}{dt} \times r' + 2m\omega \times v' + m\omega \times (\omega \times r') \tag{3}$$

$$\tau = J\dot{\omega} + \omega \times J\omega \tag{4}$$

Variable / acronym	Definition (3–element vectors expressed in accelerating, rotating coordinates of choice)
F	Vector sum of external forces
v'	Translational velocity
τ	Vector sum of external torques
r'	Position
ω	Angular velocity of chosen frame relative to nonrotating, non–accelerating frame
$\dot{\omega}$	Angular acceleration of chosen frame relative to nonrotating, non–accelerating frame

[1] Such tables are offered throughout the manuscript to aid readability.

Table 2. Table of proximal variable and acronym definitions.

The matrices of direction cosines from a prescribed rotation sequence are displayed in equations (5) and (6) and equated to an equivalent rotation matrix in equation (7) derived using the quaternions which must obey the necessary normalization condition in equation (8). In section III, "Results," attitude errors will be expressed in terms of the roll, pitch, and yaw Euler angles that were calculated using the quaternion-derived direction cosine matrix.

$$\begin{Bmatrix} X_B \\ Y_B \\ Z_B \end{Bmatrix} = \underbrace{\begin{bmatrix} 1 & 0 & 0 \\ 0 & \cos(\phi) & \sin(\phi) \\ 0 & -\sin(\phi) & \cos(\phi) \end{bmatrix}}_{\text{1 rotation (about } X'' = X_B)} \underbrace{\begin{bmatrix} \cos(\theta) & 0 & -\sin(\theta) \\ 0 & 1 & 0 \\ \sin(\theta) & 0 & \cos(\theta) \end{bmatrix}}_{\text{2 rotation (about } Y')} \underbrace{\begin{bmatrix} \cos(\psi) & \sin(\psi) & 0 \\ -\sin(\psi) & \cos(\psi) & 0 \\ 0 & 0 & 1 \end{bmatrix}}_{\text{3 Rotation (about } Z_i)} \begin{Bmatrix} X_i \\ Y_i \\ Z_i \end{Bmatrix} \tag{5}$$

$$\begin{Bmatrix} X_B \\ Y_B \\ Z_B \end{Bmatrix} = \begin{bmatrix} \cos(\theta)\cos(\psi) & \cos(\Theta)\sin(\psi) & -\sin(\theta) \\ \sin(\phi)\sin(\theta)\cos(\psi) - \cos(\phi)\sin(\psi) & \sin(\Phi)\sin(\theta)\sin(\psi) + \cos(\phi)\cos(\psi) & \sin(\phi)\cos(\theta) \\ \cos(\phi)\sin(\theta)\cos(\psi) + \sin(\phi)\sin(\psi) & \cos(\Phi)\sin(\theta)\sin(\psi) - \sin(\phi)\cos(\psi) & \cos(\phi)\cos(\theta) \end{bmatrix} \begin{Bmatrix} X_i \\ Y_i \\ Z_i \end{Bmatrix} \tag{6}$$

$$\begin{Bmatrix} X_B \\ Y_B \\ Z_B \end{Bmatrix} = \underbrace{[DCM] \begin{Bmatrix} X_i \\ Y_i \\ Z_i \end{Bmatrix}}_{\text{Equation (4)}} = \underbrace{\begin{bmatrix} 1 - 2(q_2^2 + q_3^2) & 2(q_1 q_2 + q_3 q_4) & 2(q_1 q_3 + q_2 q_4) \\ 2(q_1 q_2 + q_3 q_4) & 1 - 2(q_1^2 + q_3^2) & 2(q_2 q_3 + q_1 q_4) \\ 2(q_1 q_3 + q_2 q_4) & 2(q_2 q_3 + q_1 q_4) & 1 - 2(q_1^2 + q_2^2) \end{bmatrix}}_{\text{Quaternion Matrix}} \begin{Bmatrix} X_i \\ Y_i \\ Z_i \end{Bmatrix} \tag{7}$$

$$\underbrace{q^T q + q_4^2 = q_1^2 + q_2^2 + q_3^2 + q_4^2 = 1}_{\text{Quaterion Normalization Condition}} \tag{8}$$

Variable	Definition	Variable	Definition
ϕ	Roll attitude angle about body's x–axis	q_1	Imaginary x–coordinate of Euler axis
Θ	Pitch attitude angle about intermediate y–axis	q_2	Imaginary y–coordinate of Euler axis
ψ	Yaw attitude angle about inertial z–axis	q_3	Imaginary z–coordinate of Euler axis
DCM	Direction cosine matrix	q_4	Rotation angle about Euler axis
X_B	x–axis in the body reference frame	X_i	x–axis in the inertial reference frame
Y_B	y–axis in the body reference frame	Y_i	y–axis in the inertial reference frame
Z_B	z–axis in the body reference frame	Z_i	z–axis in the inertial reference frame

[1] Such tables are offered throughout the manuscript to aid readability.

Table 3. Table of proximal variable and acronym definitions.

The governing differential equations expressed so far will be used as the structure of self-awareness statements in deterministic artificial intelligence, and after reparameterization into standard regression form become able to facilitate optimal learning (in the 2-norm sense).

2. Deterministic artificial intelligence self-awareness statements

Self-awareness statements were first expressed by Cooper and Heidlauf in [57] as applied to nonlinear differential equations of chaotic circuits, while the specific articulation for motion mechanics was first expressed by Smeresky and Rizzo a few years later in 2020 [58].

$$F \equiv \hat{m}\ddot{x}_d + \hat{m}\frac{d\omega_d}{dt} \times r'_d + 2\hat{m}\omega_d \times v'_d + \hat{m}\omega_d \times (\omega_d \times r'_d) \tag{9}$$

$$\tau \equiv \hat{J}\dot{\omega}_d + \omega_d \times \hat{J}\omega_d \equiv [\Phi_d]\{\hat{\Theta}\} \tag{10}$$

Variable	Definition	Variable	Definition
F	Externally applied resultant force	τ	Externally applied resultant force
$\hat{m}$	Learned estimates of masses	$\hat{J}$	Learned estimates of mass moments
$\ddot{x}_d$	Desired translational acceleration	$\dot{\omega}_d$	Desired rotational acceleration
$d\omega_d/dt$	Desired rotational acceleration	ω_d	Desired angular velocity
r'_d	Desired translational position	Φ_d	Regression matrix of "knowns"
v'_d	Desired translational velocity	$\hat{\Theta}$	Regression vector of "unknowns"

[1] Such tables are offered throughout the manuscript to aid readability.

Table 4. Table of proximal variable and acronym definitions.

The key feature is to re-parameterize the system of coupled nonlinear equations into a standard regression form depicted in equation (10) noting the nature of the reparameterization is also represented in equation (9). While the manifestation of self-awareness statements for unmanned underwater vehicles in [50] merely represented five degrees of mechanical motion, the representation described here elaborates six degrees of freedom.

3. Deterministic artificial intelligence optimal learning

Optimal learning as elaborated generically by Smeresky and Rizzo in [58] is expressed in equation (11) which, together with equation (10), is the content of the attitude controller subsystem of the topology in Figure 4. Note that the final term in equation (11), δu, must be estimated by observers that are not specified in this work permitting easy identification of the *next steps in the research lineage* for formulating recommendations for future research. High-gain Luenberger observers were utilized here with no attempts made for optimization to minimize a particular reward function.

$$\{\widehat{\Theta}\} = \{\widehat{\Theta}_0\} + ([\Phi_d]^T[\Phi_d])^{-1}[\Phi_d]^T\delta u \tag{11}$$

Theorem 1 and the accompanying proof validate the optimality of the learned parameters, since the chosen learning rule is the pseudoinverse solution of the governing equations of motion formulated as self-awareness statements.

Variable	Definition	Variable	Definition
$\widehat{\Theta}$	Learned estimates	Φ_d	Regression matrix of "knowns"
$\widehat{\Theta}_0$	Initial estimate	δu	Estimated control deviation

[1] Such tables are offered throughout the manuscript to aid readability.

Table 5. Table of proximal variable and acronym definitions.

Theorem 1. Assuming mechanical motion over time will produce tall matrix with full column rank, i.e., $\mathrm{rank}(\Phi_\mathrm{d}) = \mathrm{n} \leq \mathrm{m}$. Then the pseudoinverse of Φ_d is displayed in equation (12).

$$\Phi_\mathrm{d}{}^\dagger = ([\Phi_\mathrm{d}]^\mathrm{T}[\Phi_\mathrm{d}])^{-1}[\Phi_\mathrm{d}]^\mathrm{T} \tag{12}$$

Proof of Theorem 1. Verification of four conditions for being a pseudoinverse suffices and is elaborated in equation (13):

$$\begin{aligned}
&[\Phi_d][\Phi_d]^\dagger[\Phi_d] = [\Phi_d]\cdot([\Phi_d]^T[\Phi_d])^{-1}[\Phi_d]^T\cdot[\Phi_d] = [\Phi_d]\\
&[\Phi_d]^\dagger[\Phi_d][\Phi_d]^\dagger = ([\Phi_d]^T[\Phi_d])^{-1}[\Phi_d]^T\cdot[\Phi_d]\cdot([\Phi_d]^T[\Phi_d])^{-1}[\Phi_d]^T = [\Phi_d]
\end{aligned} \tag{13}$$

$[\Phi_d][\Phi_d]^T = [\Phi_d]([\Phi_d]^T[\Phi_d])^{-1}[\Phi_d]^T$ symmetric

$[\Phi_d]^T[\Phi_d] = ([\Phi_d]^T[\Phi_d])^{-1}[\Phi_d]^T \cdot [\Phi_d] = [\mathrm{I}_n]$ symmetric

Therefore $\Phi_d{}^{\dagger} = ([\Phi_d]^T[\Phi_d])^{-1}[\Phi_d]^T$ is the pseudoinverse of $[\Phi_d]$□

4. Discretization and numerical precision

Since the assertion of self-awareness with optimal learning is validated in simulation experiments in section III, a brief discussion of errors in numerical computation is mandatory.

Simulations suffer from precision issues, particularly with nonlinear equations or coupled sets of equations. Since the governing equations elaborated in subsections II.1.–II.2. are both nonlinear and coupled, special attention is paid to numeric solver selection and computational discretization intervals using the accuracy of calculating the sums of transcendental sines and cosines as a figure of merit for numerical precision.

Table 3 displays general guidance for initial solver selection based on necessary accuracy and time-varying nature of the simulated equations. This initial solver selection guidance was used to initiate a particularized comparative analysis for selecting both solver and discretization step-size in section III.1.

Method	Solver	Problem[1]	Order of accuracy	When to use
Explicit Runge–Kutta	ode45	Nonstiff	Medium	Most of the time
	ode23	Nonstiff	Low	With crude error tolerances
Adams–Bashforth–Moulton	ode113	Nonstiff	Low to high	With stringent error tolerances
Numerical differentiation	ode15s	Stiff	Low to medium	If ode45 is slow due to stiffness
Modified Rosenbrock	ode23s	Stiff	Low	With crude error tolerances
Trapezoid rule	ode23t	Moderately stiff	Low	With crude error tolerances
Trapezoid rule with back differentiation	ode23tb	Stiff	Low	

[1] Such tables are offered throughout the manuscript to aid readability.

Table 6. An ordinary differential equation problem is stiff if the solution being sought is varying slowly, but there are nearby solutions that vary rapidly, so the numerical method must take small steps to obtain satisfactory results

III. RESULTS

The mathematical relationships in section II. were implemented in MATLAB®/SIMULINK® as depicted in Figure 4, and the simulation results are presented here in section III. Foremost, analysis is provided to justify the selection of computational solvers and discretization step-size. Transcendental functions elaborated in equation (14) were used to indicate the ability of the software to accurately perform calculations with numerical precision.

$$\{Precision\ measure\} = \left\{ \begin{Bmatrix} 1 \\ 1 \\ 1 \end{Bmatrix} - \sqrt{\left(\sin \begin{Bmatrix} \phi \\ \theta \\ \psi \end{Bmatrix} \right)^2 + \left(\cos \begin{Bmatrix} \phi \\ \theta \\ \psi \end{Bmatrix} \right)^2} \right\} \tag{14}$$

Fourth-ordered Runge–Kutta (RK) is utilized with a discretization step-size of 0.01 seconds, where iterations are displayed in Figure 5 with corresponding figures of merit displayed in Table 7. Subsequently, simulation model check-out is validated by commanding a specified navigation task displayed in Figure 6, where no specific tuning of control parameters is necessary.

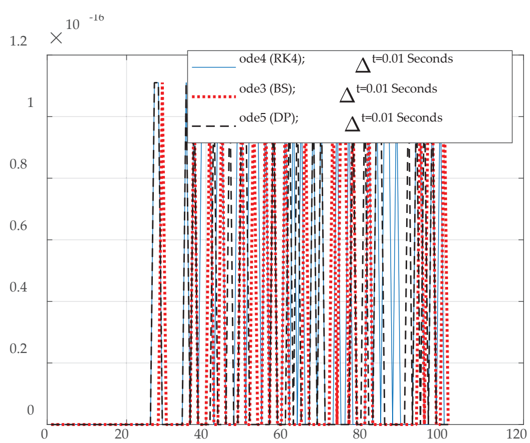

(a)

Table 7. Numerical precision for different solver schemes using MATLAB® R2022B

Step-size	Solver	Solver Type	Mean precision measure [1]
Auto	Auto	Auto Select	FAILED
0.1	ode4	4th-order RK	FAILED
0.05	ode4	4th-order RK	FAILED
0.01	ode1	Euler	FAILED
0.01	ode3	3rd-order RK	2.1×10^{-17}
0.01	ode4	4th-order RK	3.5×10^{-17}
0.01	ode5	5th-order RK	2.3×10^{-17}

[1] Machine precision = 2.2×10^{-16}; RK = Runge Kutta

(b)

Figure 5. Comparison of numeric precision

Numerical precision was determined using the calculation of the root of the sum of squares of transcendental functions (sines and cosines) of the attitude angles (on the ordinate of figure 5). Time-steps were iterated and displayed on the abscissa for different step sizes and solver schemes. Maximum error for each step-size and associated solver are displayed in Table 7 (inserted as subfigure (b) in Figure 5).

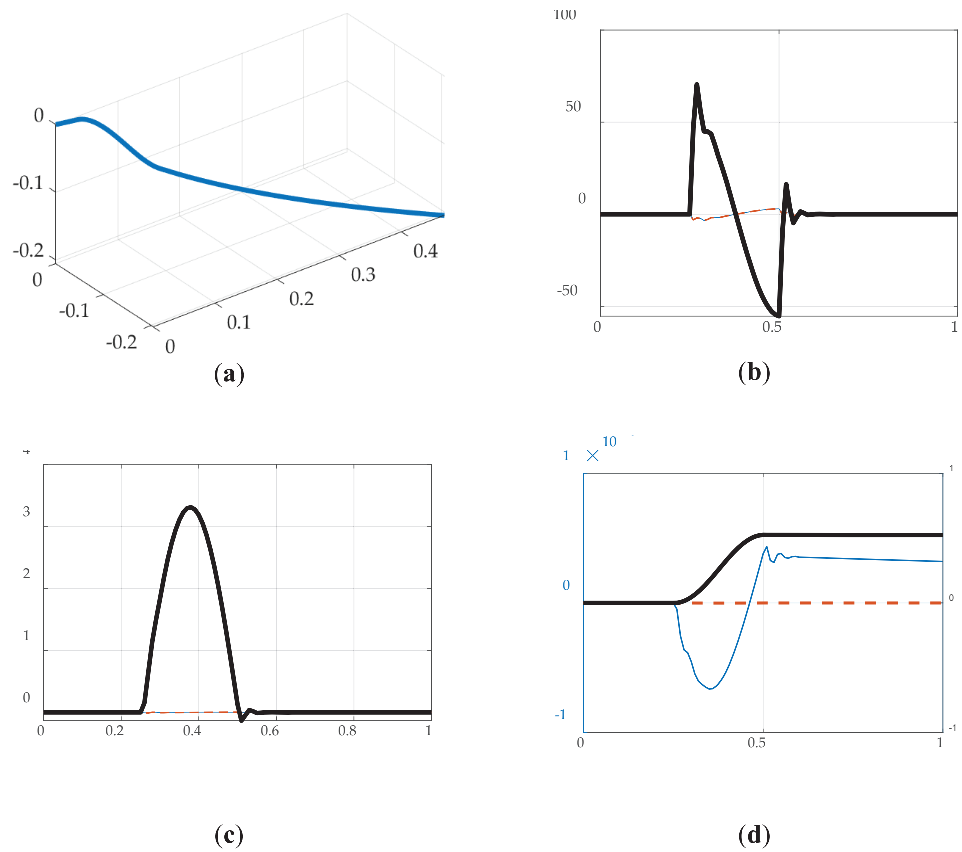

Figure 6. Validating maneuvering simulation
(a) Three-dimensional path trajectory tracking validation using the simulation depicted in Figure 4, (b) angular acceleration (radians per squared seconds) versus normalized time, (c) angular velocity (radians per second) versus normalized time, (d) rotation angle (radians) versus normalized time, where blue solid line is roll and red dashed line is pitch both measured using the left ordinant, while the solid black line is yaw (the maneuver axis) measure using the right ordinant.

This section illustrates the complexity of the six-governing coupled nonlinear differential equations. Complexity was immediately evidenced by the struggle to choose a numerical solver and discretization timestep that permitted full simulation of the commanded maneuver. Euler angle errors were used in a combined measure of numerical precision to indicate precision. Machine precision is an upper bound on the relative approximation error due to rounding in floating point arithmetic, and the measure of machine precision for the utilized computer software was achieved for the full six–degree–of–freedom simulation.

A. DISCUSSION

Autonomy of underwater vehicles can be implemented using various stochastic or deterministic artificial intelligence methods and/or hardware improvements. Many such instantiations were reviewed here: **a focus on reinforcement learning proved unimpressive**. Generally, the strongest-claimed results in most of the reviewed literature were merely akin to "effectiveness was validated" in instances lacking direct comparison to benchmark approaches. A promising method called deterministic artificial intelligence has recently appeared in several publications, ubiquitously compared to state-of-the-art methods using multiple figures of merit representing accuracy, errors, effort minimization (e.g., fuel), and computational burden. Recently published applications include unmanned underwater vehicles [54] (vehicle guidance and control [55] and actuator motor controllers [56]), aerial drone electronics [57], autonomous spacecraft guidance and control [58], and chaotic circuits (e.g., van der Pol, Lorenz, etc.) [59]. Accordingly, the creation of a baseline six-degree-of-freedom simulation was presented and validated in this present manuscript.

1. Recommended future research

The final term in equation (11), δu, must be estimated by observers that are not specified in this work permitting easy identification of the next steps in the research lineage for formulating recommendations for future research. High-gain Luenberger observers were utilized here with no attempts made for optimization. The observers are inside the attitude controller subsystem in Figure 4 and they are used to provide estimates of the control that resulted in the manifest motion. The observer gains are the only remaining portion of the proposed method that necessitates user tuning, so future efforts to utilize nonlinear observers should lead to improved system performance and additionally enhanced autonomy. Lastly, implementation in simulations and validating experiments concentrated on performing benchmark tasks such as avoidance of mines while navigating in realistic ocean currents (displayed in Figure 1 and Figure 2). A Broad Area Study has already been submitted to the FY2025 Naval Research Program sponsored by N2/N6-Information Warfare under the Topic: NPS-25-N001 Adaptive and Learning Undersea Systems.

2. Patents

While not specifically patented, the seminal expression of deterministic artificial intelligence [54] was awarded Best Paper honors [61] by the *Journal of Marine Science and Engineering*, and awards in 2021 and 2022 for Best Paper Awards in Engineering by the publisher MDPI who is among the largest publishers in the world in terms of journal article output, and is the largest publisher of open access articles. Subsequent sequels by other authors applying the methods to other vehicle systems have garnered two top-cited paper awards [62] in the journals *Applied Sciences*, Editor's Choice Article award [63] in the journal *Algorithms*, Top-cited paper [64] in the journal *Aerospace*, and the Title Story Award [65] (Highly Accessed Article) in the journal *Dynamics*. Thus, deterministic artificial intelligence seems to be a highly promising, burgeoning technique.

THIS PAGE INTENTIONALLY LEFT BLANK

APPENDIX A

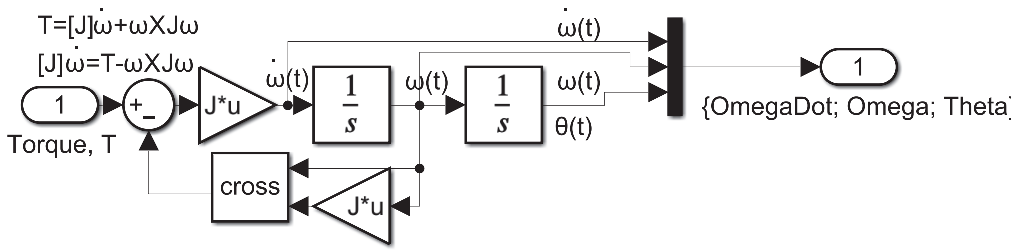

Figure 7. Euler's moment equation subsystem in Figure 4.

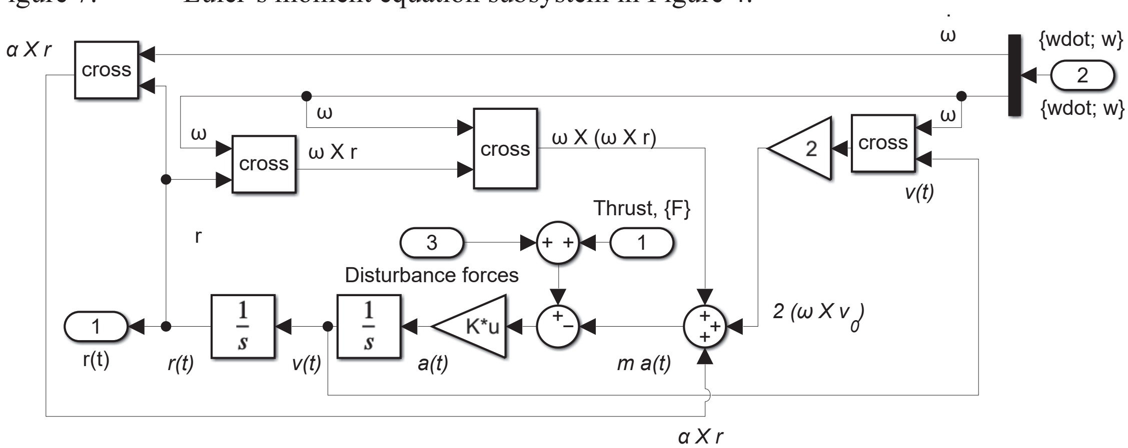

Figure 8. Newton's translation equation subsystem in Figure 4.

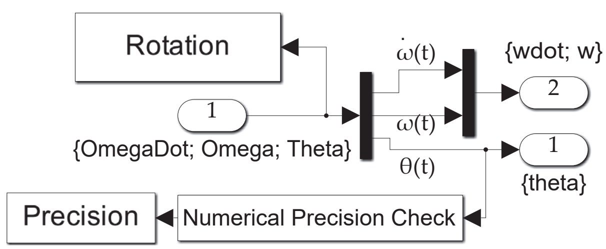

Figure 9. Rotational kinematics subsystem in Figure 4.

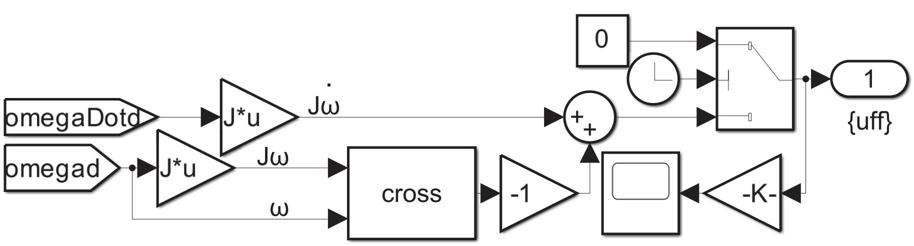

Figure 10. Attitude controller subsystem (self–awareness statements) in Figure 4.

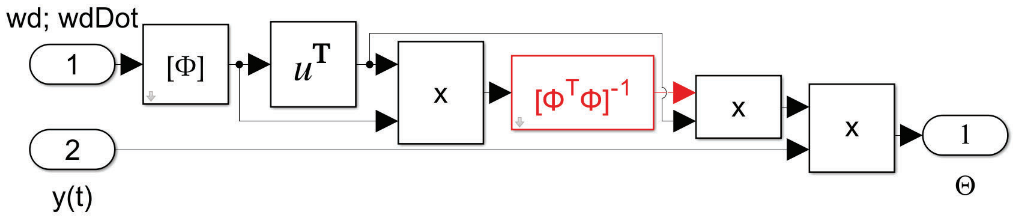

Figure 11. Attitude controller subsystem (optimal learning) in Figure 4.

LIST OF REFERENCES

[1]. Available online: https://www.defensenews.com/naval/2022/11/29/whats-ahead-for-navy-unmanned-underwater-vehicle-programs/ (Accessed June 8, 2023)

[2]. Available online: https://www.defense.gov/Contact/Help-Center/Article/Article/2762906/use-of-department-of-defense-imagery/ (Accessed June 8, 2023)

[3]. Available online: https://www.557weatherwing.af.mil/News/Article-Display/Article/2517303/machine-learning-radar-closing-the-gap-to-operations/ (Accessed June 8, 2023)

[4]. Sands, T.; Bollino, K.; Kaminer, I.; Healey, A. Autonomous Minimum Safe Distance Maintenance from Submersed Obstacles in Ocean Currents. *J. Mar. Sci. Eng.* **2018**, *6*(3), 98

[5]. Allard, Y.; Shahbazian, E. Unmanned Underwater Vehicle (UUV) Information Study; OODA Technology Inc.: Montreal, QC, Canada, 2014. Available online (accessed 30 October 2022): https://cradpdf.drdc-rddc.gc.ca/PDFS/unc199/p800838_A1b.pdf

[6]. Yang, T.C. Properties of underwater acoustic communication channels in shallow water. *J. Acoust. Soc. Am.* **2012**, *131*, 129–145.

[7]. Sinisterra, A.; Dhanak, M.; Kouvaras, N. A USV Platform for Surface Autonomy. In Proceedings of the IEEE conference OCEANS 2017, Anchorage, AK, USA, 18–21 September 2017; pp. 1–8.

[8]. Martinez, J.; Brescia, A.; Mullen, L.; Mulligan, A.; Alley, D.; Lautrup, R.; Platt, D. NIX USV platform for precision track and trail of UUV platforms, Proceedings of the SPIE Conference on Ocean Sensing and Monitoring XII, 114200O (22 April 2020), online conference doi: 10.1117/12.2565482

[9]. Cen, Y.; Liu, M.; Li, D.; Meng, K.; Xu, H. Double-Scale Adaptive Transmission in Time-Varying Channel for Underwater Acoustic Sensor Networks. *Sensors* **2021**, *21*, 2252

[10]. Savkin, A.V.; Verma, S.C.; Anstee, S. Optimal Navigation of an Unmanned Surface Vehicle and an Autonomous Underwater Vehicle Collaborating for Reliable Acoustic Communication with Collision Avoidance. *Drones* **2022**, *6*, 27.

[11]. Konoplin, A.; Yurmanov, A.; Krasavin, N.; Piatavin, P. Development of a Control System for Multilink Manipulators on Unmanned Underwater Vehicles Dynamically Positioned over Seafloor Objects. *Appl. Sci.* **2022**, *12*(3), 1666.

[12]. Liu, X.; Hu, Y.; Mao, Z.; Tian, W. Numerical Simulation of the Hydrodynamic Performance and Self-Propulsion of a UUV near the Seabed. *Appl. Sci.* **2022**, *12*(14), 6975.

[13]. Kang, J.-G.; Kim, T.; Kwon, L.; Kim, H.-D.; Park, J.-S. Design and Implementation of a UUV Tracking Algorithm for a USV. *Drones* **2022**, *6*(3), 66

[14]. Kotis, K.; Stavrinos, S.; Kalloniatis, C. Review on Semantic Modeling and Simulation of Cybersecurity and Interoperability on the Internet of Underwater Things. *Future Internet* **2023**, *15*(1), 11.

[15]. Yan, Z.; Jiang, A.; Lai, C. Adaptive Formation Control of Unmanned Underwater Vehicles with Collision Avoidance under Unknown Disturbances. *J. Mar. Sci. Eng.* **2022**, *10*(4), 516.

[16]. Yun, S.-J.; Kim, H.-G.; Park, J.-W.; Lee, H.-J.; Kim, J.-C.; Hwang, J.-H.; Choi, Y.-H.; Lee, S.-J.; Ryu, J.-K.; Suh, J.-H.; Park, J.-G. Development of a Towed Underwater Platform That Can Operate in a Marine Environment and Explore the Sea Bottom. *J. Mar. Sci. Eng.* **2022**, *10*(1), 66.

[17]. Wang, Y.; Wang, H.; Li, Q.; Xiao, Y.; Ban, X. Passive Sonar Target Tracking Based on Deep Learning. *J. Mar. Sci. Eng.* **2022**, *10*(2), 181

[18]. Yan, Z.; Jiang, A.; Lai, C.; Li, H. Velocity-Free Formation Control and Collision Avoidance for UUVs via RBF: A High-Gain Approach. *Electronics* **2022**, *11*(8), 1170

[19]. Zhu, B.; Liu, L.; Zhang, L.; Liu, M.; Duanmu, Y.; Chen, Y.; Dang, P.; Li, J. A Variable-Order Fuzzy Logic Controller Design Method for an Unmanned Underwater Vehicle Based on NSGA-II. *Fractal Fract.* **2022**, *6*(10), 577.

[20]. Wu, X.; Gao, Z.; Yuan, S.; Hu, Q.; Dang, Z. A Dynamic Task Allocation Algorithm for Heterogeneous UUV Swarms. *Sensors* **2022**, *22*(6), 2122

[21]. Wang, S.; Sun, J.; Zhao, B.; Yun, Y.; Huang, B. Numerical Study on the Interaction between Ocean Current Power Generator and Unmanned Underwater Vehicle. *J. Mar. Sci. Eng.* **2022**, *10*(12), 1869.

[22]. Chen, M.; Liu, J.; Si, Q.; Liang, Y.; Jin, Z.; Yuan, J. Investigation into the Hydrodynamic Noise Characteristics of Electric Ducted Propeller. *J. Mar. Sci. Eng.* **2022**, *10*(3), 378.

[23]. Xu, L.; Huang, J.; Zhang, H.; Liao, B. Direction of Arrival Estimation of Acoustic Sources with Unmanned Underwater Vehicle Swarm via Matrix Completion. *Remote Sens.* **2022**, *14*(15), 3790.

[24]. Qin, J.; Li, M.; Li, D.; Zhong, J.; Yang, K. A Survey on Visual Navigation and Positioning for Autonomous UUVs. *Remote Sens.* **2022**, *14*(15), 3794.
[25]. Lambertini, A.; Menghini, M.; Cimini, J.; Odetti, A.; Bruzzone, G.; Bibuli, M.; Mandanici, E.; Vittuari, L.; Castaldi, P.; Caccia, M.; De Marchi, L. Underwater Drone Architecture for Marine Digital Twin: Lessons Learned from SUSHI DROP Project. *Sensors* **2022**, *22*(3), 744.
[26]. Khawaja, W.; Semkin, V.; Ratyal, N.I.; Yaqoob, Q.; Gul, J.; Guvenc, I. Threats from and Countermeasures for Unmanned Aerial and Underwater Vehicles. *Sensors* **2022**, *22*(10), 3896.
[27]. Xie, Y.; Bore, N.; Folkesson, J. Sidescan Only Neural Bathymetry from Large-Scale Survey. *Sensors* **2022**, *22*(14), 5092.
[28]. Yang, H.; Xu, Z.; Jia, B. An Underwater Positioning System for UUVs Based on LiDAR Camera and Inertial Measurement Unit. *Sensors* **2022**, *22*(14), 5418.
[29]. Sola, Y.; Le Chenadec, G.; Clement, B. Simultaneous Control and Guidance of an AUV Based on Soft Actor–Critic. *Sensors* **2022**, *22*(16), 6072.
[30]. Zhang, Z.; Mi, W.; Du, J.; Wang, Z.; Wei, W.; Zhang, Y.; Yang, Y.; Ren, Y. Design and Implementation of a Modular UUV Simulation Platform. *Sensors* **2022**, *22*(20), 8043
[31]. Shi, Z.; Tan, X.; Wang, Y.; Lv, P.; Zou, Y.; Wan, X.; Lv, K.; Li, B.; Duan, H.; Li, H. Experimental Investigation of High Speed Cross-Domain Vehicles with Hydrofoil. *J. Mar. Sci. Eng.* **2023**, *11*(1), 152.
[32]. Listewnik, K.J.; Aftewicz, K. Rotary 3D Magnetic Field Scanner for the Research and Minimization of the Magnetic Field of UUV. *Sensors* **2023**, *23*(1), 345.
[33]. Park, B.H.; Choi, H.B.; Seo, H.-S.; Je, Y.; Yi, H.; Park, K.K. Development of Multilayer Transducer and Omnidirectional Reflection Model for Active Reflection Control. *Sensors* **2023**, *23*(1), 521.
[34]. Kang, J.-G.; Kim, T.; Kwon, L.; Kim, H.-D.; Park, J.-S. Design and Implementation of a UUV Tracking Algorithm for a USV. *Drones* **2022**, *6*(3), 66.
[35]. Alrayes, F.S.; Alotaibi, S.S.; Alissa, K.A.; Maashi, M.; Alhogail, A.; Alotaibi, N.; Mohsen, H.; Motwakel, A. Artificial Intelligence-Based Secure Communication and Classification for Drone-Enabled Emergency Monitoring Systems. *Drones* **2022**, *6*(9), 222.
[36]. Cho, H.; Jeong, S.-K.; Ji, D.-H.; Tran, N.-H.; Vu, M.T.; Choi, H.-S. Study on Control System of Integrated Unmanned Surface Vehicle and Underwater Vehicle. *Sensors* **2020**, *20*(9), 2633.
[37]. Raigoza, K.; Sands, T. Autonomous Trajectory Generation Comparison for De-Orbiting with Multiple Collision Avoidance. *Sensors* **2022**, *22*(8), 7066.
[38]. Koo, S.M.; Travis, H.; Sands, T. Impacts of Discretization and Numerical Propagation on the Ability to Follow Challenging Square Wave Commands. *J. Mar. Sci. Eng.* **2022**, *10*(3), 419.
[39]. Bourgeois, B.; McDowell, P. UUV Teams For Deep Water Operations. *Underwater Intervention 2001* conference, New Orleans, Louisiana, February 2002. Available online: https://apps.dtic.mil/sti/citations/ADA400686 (accessed on 23 October 2022).
[40]. Miller, D. Design of a small, cheap UUV for under-ship inspection and salvage. Proceedings of Symposium on Autonomous Underwater Vehicle Technology, 02-06 June 1996, Monterey, USA. pp. 18-20.
[41]. Eldred, R.; Lussier, J.; Pollman, A. Design and Testing of a Spherical Autonomous Underwater Vehicle for Shipwreck Interior Exploration. *J. Mar. Sci. Eng.* **2021**, *9*(3), 320.
[42]. Eldred, R.; Van Bossuyt, D.L. Preliminary Design and Testing of a Resetting Combination Anchor, Antenna, and Tether Mechanism for a Spherical Autonomous Underwater Vehicle. *Appl. Sci.* **2022**, *12*, 5072.
[43]. Rosynski, M.; Buşoniu, L. A Simulator and First Reinforcement Learning Results for Underwater Mapping. *Sensors* **2022**, *22*(14), 5384.
[44]. He, A.; Dong, L.; Sun, C.; Wang, J. Asynchronous Multithreading Reinforcement-Learning-Based Path Planning and Tracking for Unmanned Underwater Vehicle. *IEEE Trans. Sys., Man, Cyber: Sys.* **2022**, *52*(5), 2757-2769.
[45]. Wang, Z.; Wen, Z.; Xia, Q.; Cai, W. Deep Reinforcement Learning Based Multi-UUV Cooperative Control for Target Capturing. In Proceedings of the 2022 IEEE Intl Conf on Dependable, Autonomic and Secure Computing, Intl Conf on Pervasive Intelligence and Computing, Falerna, Italy, 12-15 September 2022
[46]. Wang, D., He, B., Shen, Y. et al. A Modified ALOS Method of Path Tracking for AUVs with Reinforcement Learning Accelerated by Dynamic Data-Driven AUV Model. *J In-tell Robot Syst.* **2022**, *104*(49).

[47]. Wang, G.; Wei, F.; Jiang, Y.; Zhao, M.; Wang, K.; Qi, H. A Multi-AUV Maritime Target Search Method for Moving and Invisible Objects Based on Multi-Agent Deep Reinforcement Learning. *Sensors* **2022**, *22*(21), 8562.
[48]. Duan, K.; Fong, S. Chen, C. Reinforcement learning based model-free optimized trajectory tracking strategy design for an AUV, *Neurocomputing* **2022**, 469, 289-297.
[49]. Masmitja, I.; Martin, M.; Katija, K.; Gomariz, S.; Navarro, J. A reinforcement learning path planning approach for range-only underwater target localization with autonomous vehicles, In Proceedings of the 2022 IEEE 18th International Conference on Automation Science and Engineering (CASE), Mexico City, Mexico, 20-24 August 2022
[50]. Cao, Y.; Kou, Y.; Li, Z. Xu, A. Autonomous Maneuver Decision of UCAV Air Combat Based on Double Deep Q Network Algorithm and Stochastic Game Theory *Int. J. Aero. Eng.* **2023**, 3657814.
[51]. Bu, F.; Luo, H.; Ma, S.; Li, X.; Ruby, R.; Han, G. AUV-Aided Optical—Acoustic Hybrid Data Collection Based on Deep Reinforcement Learning. *Sensors* **2023**, *23*(2), 578.
[52]. Lu, W.; Cheng, K.; Hu, M. Reinforcement Learning for Autonomous Underwater Vehicles via Data-Informed Domain Randomization. *Appl. Sci.* **2023**, *13*(3), 1723.
[53]. McDowell, P.; Iyengar, S.; Gendron, M.; Bourgeois, B.; Sample, J. Control/Learning Architectures for Use in Robots Operating in Unstructured Environments. Proceedings of the Southern Conference on Computing. October 26-28, 2000. The University of Southern Mississippi, Hattiesburg, Mississippi, USA.
[54]. Sands, T. Development of Deterministic Artificial Intelligence for Unmanned Underwater Vehicles (UUV). *J. Mar. Sci. Eng.* **2020**, *8*(8), 578
[55]. Osler, S.; Sands, T. Controlling Remotely Operated Vehicles with Deterministic Artificial Intelligence. *Appl. Sci.* **2022**, *12*(6), 2810.
[56]. Shah, R.; Sands, T. Comparing Methods of DC Motor Control for UUVs. *Appl. Sci.* **2021**, *11*(11), 4972.
[57]. Xu, J.; Sands, T. Autonomous Drone Electronics Amplified with Pontryagin-Based Optimization. *Electronics* **2023**, *12*(11), 2541.
[58]. Sandberg, A.; Sands, T. Autonomous Trajectory Generation Algorithms for Spacecraft Slew Maneuvers. *Aerospace* **2022**, *9*(3), 135.
[59]. Cooper, M.; Heidlauf, P.; Sands, T. Controlling Chaos—Forced van der Pol Equation. *Mathematics* **2017**, *5*(4), 70.
[60]. Smeresky, B.; Rizzo, A.; Sands, T. Optimal Learning and Self-Awareness Versus PDI. *Algorithms* **2020**, *13*(1), 23.
[61]. Available online: https://www.mdpi.com/journal/jmse/awards/906 (accessed July 27, 2023).
[62]. Available online: https://www.mdpi.com/about/announcements/4440 (accessed July 27, 2023).
[63]. Available online: https://twitter.com/Algorithms_MDPI/status/1398115606562361346?s=20 (accessed July 27, 2023).
[64]. Available online: https://twitter.com/DrTimothySands/status/1678187671678509056?s=20 (accessed July 27, 2023).
[65]. Available online: https://twitter.com/DrTimothySands/status/1678186215684595715?s=20 (accessed July 27, 2023).

THIS PAGE INTENTIONALLY LEFT BLANK

INITIAL DISTRIBUTION LIST

1. Defense Technical Information Center
   Ft. Belvoir, Virginia

2. Dudley Knox Library
   Naval Postgraduate School
   Monterey, California

3. Research Sponsored Programs Office, Code 41
   Naval Postgraduate School
   Monterey, CA 93943

4. Daniel Breedlove
   Department of the Navy, Office of Naval Intelligence
   Washington, DC 20395-5720